Probability distributions of particle hop distance and travel time over equilibrium mobile bedforms

Thomas C. Ashley[1], Robert C. Mahon[2], Suleyman Naqshband[3], Kate C.P. Leary[4], Brandon McElroy[1]

[1]Department of Geology and Geophysics, University of Wyoming, Laramie, WY
[2]Department of Earth and Environmental Sciences, University of New Orleans, New Orleans, LA
[3]Department of Environmental Sciences, Wageningen University, Wageningen, Netherlands
[4]Department of Geography, UC Santa Barbara, Santa Barbara, CA

Key Points:

- Particle travel times over bedforms are exponentially-distributed as proposed for planar beds.
- Streamwise and lateral hop distances over bedforms are not Weibull-distributed as proposed for planar beds.
- Bedforms increase the variance in streamwise and lateral hop distances and increase diffusive-like transport.

Corresponding author: Thomas C. Ashley, tashley22@gmail.com

Abstract

The joint probability distribution of streamwise particle hop distance, lateral particle hop distance, and travel time constrains the relationships between topographic change and sediment transport at the granular scale. Previous studies have investigated the ensemble characteristics of particle motions over plane-bed topography, however it is unclear whether reported distributions remain valid when bedforms are present. Here, we present measurements of particle motion over bedform topography obtained in a laboratory flume and compare these to particle motions over plane-bed topography with otherwise similar conditions. We find substantial differences in particle motion in the presence of bedforms that are relevant to macroscopic models of sediment transport. Most notably, bedforms increase the standard deviation of streamwise and lateral hop distances relative to the mean streamwise hop distance. This implies that bedforms increase the streamwise and lateral diffusion lengths and, equivalently, increase diffusive-like fluxes.

1 Introduction

The joint probability distribution of particle hop distance and travel time is the centerpiece of the entrainment form of the Exner equation, a probabilistic statement of mass conservation that encapsulates the relationship between granular sediment motion and topographic change (Tsujimoto, 1978; Ancey, 2010; Furbish et al., 2012; Pelosi & Parker, 2014). Considerable attention has been devoted to the problem of discerning the forms of the associated marginal distributions and predicting their parameters or moments under steady, uniform macroscopic flow conditions (Abbott & Francis, 1977; Lajeunesse et al., 2010; Fathel et al., 2015; Furbish et al., 2016; HosseiniSadabadi et al., 2019; Liu et al., 2019). This objective represents an important step toward the development of models for large-scale fluvial morphodynamics that are consistent with the physics of grain-scale sediment transport.

Likely forms for the marginal probability distributions of particle hop distances and travel times can be obtained from simple assumptions about particle motion through statistical-mechanical arguments (Furbish & Schmeeckle, 2013; Furbish et al., 2016). These authors suggest that travel times are exponentially distributed while streamwise and absolute lateral hop distances follow a Weibull distribution with shape parameter $0.5 \leq k < 1$, neglecting the small fraction of particles that move in the upstream direction. Previous experimental measurements of particle motion confirm these predictions for uniform flow conditions over a flat streambed (Lajeunesse et al., 2010; Fathel et al., 2015; Campagnol et al., 2015; Furbish et al., 2016; Liu et al., 2019; Wu et al., 2020). This still leaves a gap in understanding for the wide range of conditions under which the coupled motion of fluid and sediment amplifies small perturbations in bed elevation leading to the development of ripples and dunes (Van Den Berg & Van Gelder, 1993; Southard & Boguchwal, 1990; García, 2008). We therefore seek to determine the forms of these distributions in the presence of equilibrium mobile bedforms.

The processes governing growth, coarsening, and subsequent dynamical behavior of bedforms involve a continual feedback between topography, flow, and sediment transport (Southard & Dingler, 1971; Costello, 1974; McLean, 1990; Best, 1992; Mclean et al., 1994; Venditti et al., 2005a, 2006; Coleman et al., 2006; Coleman & Nikora, 2011; Charru et al., 2013). A rich literature related to flow over bedforms reveals persistent zones of flow acceleration, expansion, and separation which modulate the bed stress and transport fields (Mclean et al., 1994; Maddux, Nelson, & McLean, 2003; Maddux, McLean, & Nelson, 2003; Best, 2005, 2009; Muste et al., 2016; Kwoll et al., 2017; Naqshband et al., 2017). Only recently have researchers begun to examine the effects of this interaction on particle kinematics through particle tracking and acoustic techniques. Experimental results indicate that instantaneous quantities like particle activity and velocity vary systematically in relation to topographic position while retaining probability dis-

tributions similar to those observed under plane-bed conditions (Wilson & Hay, 2016; Leary & Schmeeckle, 2017; Tsubaki et al., 2018; Terwisscha van Scheltinga et al., 2019). What remains unclear is how bedforms influence Lagrangian integral quantities like particle hop distance and travel time.

The purpose of this paper is to clarify how bedforms influence time-integrated particle behavior by comparing observations of particle motion over bedforms and plane-bed topography. We consider intermediate-timescale hops, defined as periods of continuous motion separated by periods of rest (*sensu* Nikora et al., 2001; Ballio et al., 2018). Here, we present the results of experiments designed to reveal differences in the probability distributions of particle hop distance and travel time over equilibrium mobile bedforms compared with plane-bed topography. We focus on properties that are relevant to macroscopic transport to determine whether existing theory developed for plane-bed topography provides a suitable description of particle motion when bedforms are present on the bed.

2 Theory

The topography of a granular bed evolves through the processes of particle entrainment and disentrainment. Each entrainment or disentrainment event produces a small change in bed elevation which, averaged over time, results in macroscopic topographic change. This notion underlies the entrainment form of Exner equation (Tsujimoto, 1978; Parker et al., 2000; Furbish et al., 2012), expressing the time rate of change of bed elevation η (L) at time t, streamwise position x and cross-stream position y in terms of the difference between the volumetric particle entrainment rate E (LT^{-1}) and disentrainment rate D (LT^{-1}) per unit bed area:

$$c_b \frac{\partial \eta}{\partial t}(t,x,y) = -E(t,x,y) + D(t,x,y). \tag{1}$$

Here, c_b (-) is the concentration of particles in the bed.

Paired entrainment and disentrainment events are explicitly linked through the motion of individual particles, defining a spatiotemporal displacement vector with components of streamwise hop distance L_x (L), lateral hop distance L_y (L), and travel time T_p (T). Because these quantities are defined in terms of particle exchanges with the bed, they also form the basis for the relationship between sediment transport and topographic change. This statement can be demonstrated by invoking the master equation to rewrite $D(t,x,y)$ as

$$\begin{aligned} D(t,x,y) \quad = \quad & \int_0^\infty \int_{-\infty}^\infty \int_0^\infty E(x-L_x, y-L_y, t-T_p) \\ & f_{T_p,L_x,L_y}(T_p, L_x, L_y; t-T_p, x-L_x, y-L_y)\, dT_p dL_x dL_y, \end{aligned} \tag{2}$$

where $f_{T_p,L_x,L_y}(T_p, L_x, L_y; t, x, y)$ is the joint probability distribution of streamwise hop distance, lateral hop distance, and travel time of particles entrained at (t,x,y). Equation (2) (Tsujimoto, 1978; Furbish et al., 2012) is fundamentally nonlocal in that it integrates conditions over space and time, however it can be approximated in terms of local variables as a Fokker-Planck equation (Furbish et al., 2012, 2017), given by

$$\begin{aligned} c_b \frac{\partial \eta}{\partial t}(t,x,y) = \quad & -\frac{\partial}{\partial x}(E\overline{L_x}) - \frac{\partial}{\partial y}(E\overline{L_y}) - \frac{\partial}{\partial t}(E\overline{T_p}) \\ & + \frac{1}{2}\frac{\partial^2}{\partial x^2}(E\overline{L_x^2}) + \frac{1}{2}\frac{\partial^2}{\partial y^2}(E\overline{L_y^2}) + \frac{1}{2}\frac{\partial^2}{\partial x \partial y}(E\overline{L_x L_y}) \end{aligned} \tag{3}$$

where overbars denote ensemble averages. This approximation is valid as long as the marginal probability distributions of hop distance and travel time have finite first and second moments and as long as the spatiotemporal scales of particle motion are small relative to

the scales of change in flow conditions (Furbish et al., 2012). The one dimensional fluxes q_x ($\mathrm{L^2T^{-1}}$) and q_y ($\mathrm{L^2T^{-1}}$) are obtained from (3) by assuming conditions are approximately steady in time and uniform in one spatial dimension. Noting that the variance is equal to the mean squared hop distance minus the squared mean, (i.e. $\sigma^2_{L_x} = \overline{L_x^2} - \overline{L_x}^2$), the one dimensional fluxes are given by

$$q_x(t,x,y) = E\overline{L_x} - \frac{1}{2}\frac{\partial}{\partial x}E\overline{L_x}^2 - \frac{1}{2}\frac{\partial}{\partial x}E\sigma^2_{L_x} \tag{4}$$

and

$$q_y(t,x,y) = E\overline{L_y} - \frac{1}{2}\frac{\partial}{\partial y}E\overline{L_y}^2 - \frac{1}{2}\frac{\partial}{\partial x}E\sigma^2_{L_y}. \tag{5}$$

Here, the first two terms comprise an advective-like flux consisting of a local term that is equal to the total flux under uniform transport conditions, and a nonlocal term that accounts for spatial variability in particle entrainment rate and mean hop distance. The third term is like a diffusive flux in that it is driven by the variance in particle hop distance. This interpretation differs from previous studies, reflecting the decomposition of the raw variance (i.e. $\overline{L_x^2}$) into terms containing the squared mean and variance. Under this interpretation, the squared coefficient of variation (the ratio of the standard deviation to the mean) of particle hop distances is like an inverse Peclet number in that it scales the relative propensity for diffusion-like and advection-like transport. This idea is fully discussed in Section 4.4).

The objective of this paper is to reveal the manner in which bedforms influence the marginal probability distribution of particle travel time $f_{T_p}(T_p)$, streamwise hop distance $f_{L_x}(L_x)$ and lateral hop distance $f_{L_y}(L_y)$. This work is primarily motivated by macroscopic morphodynamic modeling problems (e.g., Abramian et al., 2019) for which the most important features of these distributions are the statistical moments contained in Equations (3), (4) and (5). We consider multiple indicators of distribution fit, however we place special emphasis on those which pertain to the estimation of these moments. Results are interpreted in the context of probability distribution models proposed by Fathel et al. (2015) which are consistent with various mechanical constraints (Furbish et al., 2016) as well as with empirical constraints imposed by an extensive dataset of particle motion over plane-bed topography (Roseberry et al., 2012). These distributions exist on the domain from zero to infinity and thus ignore hops in the upstream direction. They also have thin tails and fixed coefficients of variation, implying that the propensity for diffusion-like transport varies in proportion to the advective component of flux across a wide range of conditions as discussed in more detail below. We aim to determine the extent to which the constraints that derive from the forms of these distributions provide a realistic foundation for modeling macroscopic sediment transport phenomena when bedforms are present.

3 Experiments

3.1 Overview

In order to compare the ensemble statistics of particle motions that are characteristic of plane-bed and bedform topography, we conducted two flume experiments differentiated primarily by the presence or absence of equilibrium bedforms. For each experiment we recorded videos of fluorescent tracer particles that were used to construct empirical distributions of particle hop distance and travel time. In considering fixed distributions of these quantities, we appeal to the idea of an ensemble of nominally identical systems first described by Gibbs (1902) and elaborated recently with respect to bedload transport by Furbish et al. (2012). We designed our experiments so that the distributions measured over a finite temporal and spatial domain may be assumed to be equivalent to the instantaneous ensemble distribution at any position and time. This assumption is reasonable as long as the macroscopic average conditions are steady and uniform over the domain of data collection.

Previous studies show that particle activity and velocity exhibit conditional dependence on local topographic configuration (Wilson & Hay, 2016; Leary & Schmeeckle, 2017; Tsubaki et al., 2018; Terwisscha van Scheltinga et al., 2019). Because particle hops integrate instantaneous quantities over time, it follows that particle hop distance and travel time are also likely to exhibit similar conditional dependence. In order to ensure that measured distributions reflect ensemble probability distributions characteristic of macroscopic flow conditions, measured particle motions would ideally contain a sample that is representative of all possible microconfigurations of flow and topography. In practice, this means that particle hops should be measured over spatiotemporal scales that are much larger than those of significant autocorrelation in flow velocity and bed elevation. Due to practical limitations, this was not possible for the bedform condition: particle motions were recorded over a small region of the bed with streamwise and cross-stream dimensions comparable to the bedform lengthscale which we assume is similar to the autocorrelation lengthscale of topography (Nordin, 1971; Nikora et al., 1997). Nonetheless, we posit that these data are sufficient to reveal important features of particle motion over bedforms. We report distributions sampling hops originating on both stoss and lee regions of a single bedform, roughly in proportion to the relative entrainment rates in these regions. For additional discussion of this point, see Section 4.5.

3.2 Description of Experiments

Experiments were conducted in a 7.2 m long $\times$ 0.29 m wide flume capable of recirculating both sediment and water. Bedforms were allowed to develop under constant flow conditions over a period of 48 hours, at which point particle motions were recorded using a downward-looking camera. Plane-bed conditions were then achieved by manually grading the bed using a plastic paddle, and particle motions were recorded again. Flume boundary conditions remained constant throughout this procedure: water discharge was 18 L/s, the flume slope was 0.001, and flow depth at the outlet was set to approximately $H = 0.16$ m. The mean flow velocity was $U = 0.39$ m/s, and the Froude number was $Fr = U/\sqrt{gH} = 0.31$.

The bed material had a median diameter of 330 μm and median settling velocity $\omega_s = 4.4$ cm/s. The base-2 logarithmic standard deviation was 0.69 (68% of the bed material was within a multiplicative factor of $2^{0.69} = 1.61$ of the mean). This is typical of hydraulically-sorted natural sediment in fluvial systems, but is a significant departure from the single-grain size experiments reported in previous studies. The implications of this difference are discussed in section 4.2.

Particle motions were measured using videos of fluorescent tracer particles. To this end, a small fraction of the bed material was removed from the flume and coated with a thin layer of fluorescent paint. Approximately 30 cm^3 (including pore space) of tracer particles were added back into the flume and allowed to mix with the unpainted bed material over a period of several weeks of continuous run time under a range of flow conditions. The thickness of sediment within the flume was approximately 8 cm such that the total volume of sediment in the flume including pore space was approximately 170000 cm^3 and tracer particles composed an estimated 0.017 % of the bed material. For comparison, the tracer particle percentage estimated by comparing the tracer particle flux and the bedform bedload flux (discussed below) is 0.019 %. Particles were illuminated with black lights (GE Black Light Blue bulbs, peak wavelength = 368 nm) through the side windows of the flume test reach (Figure 1a, 1b), which increased the contrast of tracer particles against the bed and facilitated consistent tracking (Naqshband et al., 2017). We assume this procedure provides an unbiased sample of complete particle hops representing the full distribution of particle sizes.

Acoustic measurements of the near-bed flow velocity profile were collected over equilibrium bedforms to compute the bed stress condition (Bagherimiyab & Lemmin, 2013;

Le Bouteiller & Venditti, 2015). The sidewall-corrected shear velocity was $u_* = 2.4$ cm/s. This produced bedload dominated bedforms with a suspension number (the ratio of shear velocity to sediment settling velocity) of 0.54. For comparison, the unit bedload flux estimated from bedform migration using the bedform bedload equation of Simons et al. (1965) was $q_b = 4.1 \times 10^{-7}$ m^2/s. Applying the Wong and Parker (2006) bedload equation and solving for stress suggests that the effective shear velocity (i.e. skin friction) driving sediment transport was $u_{*sk} = 1.8$ cm/s. This is consistent with the notion that pressure differences across a bedform reduce the bedload transport rate associated with a specified average bed stress.

Although fluid velocities were not measured directly for the plane-bed condition, we may generate an estimate of the shear velocity by comparing the relative magnitudes of the tracer particle flux (discussed below) using the Wong and Parker (2006) bedload equation. The tracer particle flux for the plane-bed experiment was 2.1 particles per second per meter width. The bedload flux is estimated to be 1.9×10^{-7} m^2/s leading to an estimated shear velocity of $u_* = 1.7$ cm/s and a suspension number of 0.38. We emphasize that this estimate requires substantial assumptions and is reported here as a best-guess to contextualize our experiments. However, the specific values of the shear velocity are not central to any of the theoretical developments or interpretations presented below.

Characteristic scales of bedform topography were computed from one-dimensional scans obtained using an ultrasonic profiler mounted to a moving cart. Equilibrium bedforms had a characteristic height $H_c = 1.5$ cm, a characteristic length $L_c = 16$ cm, and a characteristic migration velocity $V_c = 0.50$ cm/minute. Bedform height was determined using $H_c = 2\sqrt{2}\sigma_\eta$ where σ_η is the standard deviation of bed elevation (McElroy, 2009). L_c was determined from the spectral centroid of the bed profile and V_c was determined from the maximum of the cross-correlation function of successive scans (Van Der Mark & Blom, 2007). The characteristic evolution timescale of bed elevation η computed as $T_\eta = \eta/(\partial_\eta/\partial_t)$, was approximately 8 minutes, such that topography is effectively fixed within the ten-second data collection intervals.

Videos of particle motion were recorded using a submerged downward-looking camera mounted near the centerline of the flume with the lens approximately 15 centimeters from the bed. Videos were collected at a resolution of 1920 by 1080 pixels and at a frame rate of 30 frames per second. This window covered a streamwise distance of 12.2 cm, and a cross-stream distance of 21.7 cm. Two ten-second intervals from each video were used for this analysis. Image registration and rectification were performed using OpenCV in Python (Bradski, 2000) Particles were digitized manually using TrackMate (Tinevez et al., 2017), an open-source particle tracking package for ImageJ (Schindelin et al., 2012; Rueden et al., 2017). All particles that moved during each interval were tracked for their entire visible path, including rest times (Figure 1).

The position of the particle centroid was tracked to within roughly one pixel such that the total uncertainty in each estimate of particle hop distance is roughly 0.022 cm (or one pixel at the start and beginning of each hop). Note that this is comparable to the median particle diameter. The uncertainty in each particle hop distance is approximately 6.25% of the mean hop distance in the plane-bed experiment and 9.5% of the mean hop distance in the bedform experiment. This error may be positive or negative such that it is unlikely to bias estimates of the mean hop distance. In principle, this type of uncertainty could result in a positive bias in estimates of the variance by adding normally distributed noise, however the magnitude of this effect is small and equivalent for both experiments. As a result, it is ignored in the analysis presented below.

The timing of the end and beginning of particle motions can be constrained to within one frame (0.033 s). Assuming perfect detection of particle motion, the measured hop duration will always be greater than or equal to the true hop duration because motion

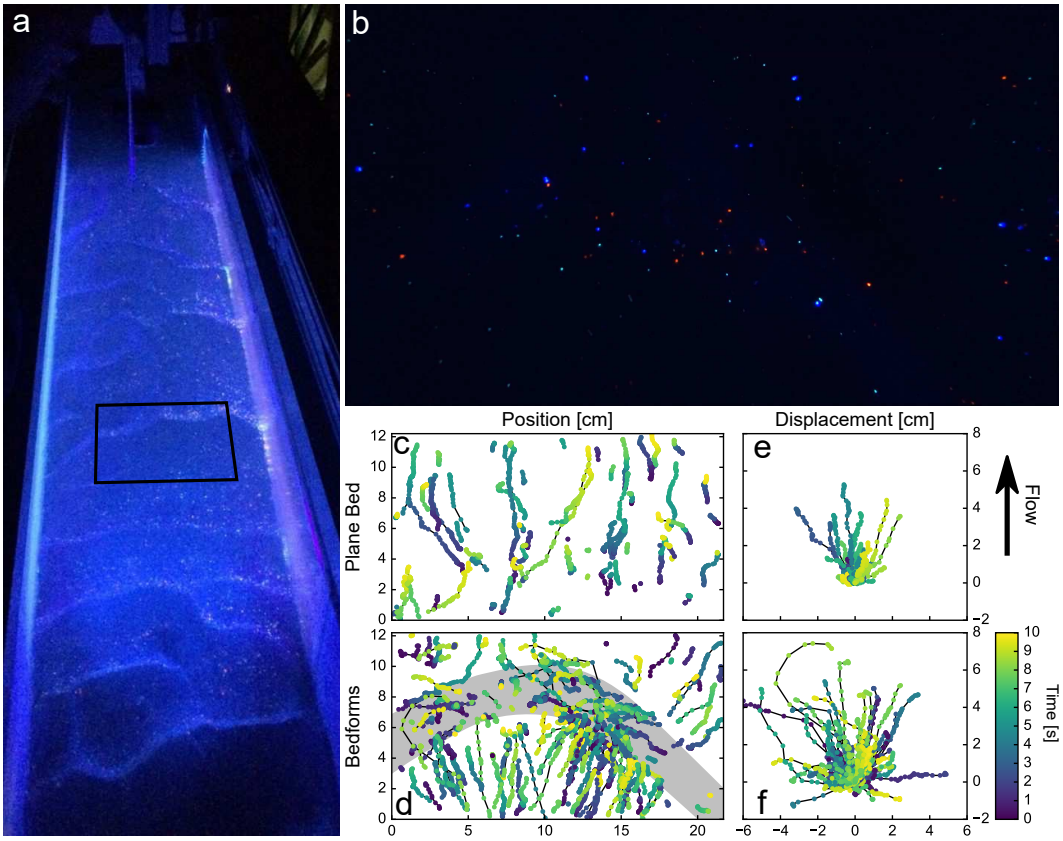

Figure 1. Experimental setup and tracked particle motions. (a) Oblique view of flume with bedforms. Black box indicates the approximate region of the bed where videos of fluorescent tracer particles were recorded. (b) Still image from video of fluorescent tracer particles during the bedform condition. Flow is from bottom to top. (c) Tracked particle motions over plane-bed and (d) bedform topography. Grey region in (d) indicates the position of a bedform lee face. Note that the particle transport direction exhibits conditional dependence on topographic configuration in the vicinity of the particle that is discussed in more detail in section 4.1. (e) Visualization of particle displacements over plane-bed and (f) bedform topography. Topographic effects manifest as qualitative differences in between (e) and (f) in the ensemble limit.

will always be registered as starting the frame before motion begins and ending the frame after motion ends. This effect will introduces a positive bias to empirical estimates of the mean travel time if the particle is assumed to be moving for the full duration over which motion is observed. Correcting for this bias is not trivial and depends on assumptions about the underlying distribution of particle travel times, however we note that the effect on the computed moments is small, biasing the estimate of the mean travel time by approximately one frame time and introducing essentially no bias to the estimate of the variance. A moderate bias correction does not influence the primary findings of this paper and is not performed here.

3.3 Definition of a Particle Hop

The concept of a complete particle "hop" follows from the notion that particles may occupy one of two mutually exclusive states: motion and rest (HosseiniSadabadi et al., 2019). This distinction is critical to the interpretation of particle-kinematic statements

of sediment mass conservation, namely, the divergence and entrainment forms of the Exner equation. However, differentiating between active and stationary particles is not straightforward: grains on the bed surface may wiggle in place without moving appreciably and may accumulate significant displacements over long timescales due to granular creep (Houssais et al., 2015). In fact, granular transport occurs via numerous phases (Houssais & Jerolmack, 2017); the binary view of mobility is merely a convenience adopted to delineate highly disparate scales of particle velocity and flux for the purposes of mathematical abstraction.

This reasoning suggests that particles on or below the bed surface are not truly stationary in the sense that they have detectable mean velocities averaged over long timescales. Consequently, empirical studies of particle motion which attempt to differentiate between mobile and immobile grains do so according to criteria that, despite their intuitive appeal, lack clear physical justification (HosseiniSadabadi et al., 2019). For example, particles are often treated as mobile when their velocity exceeds a threshold value that is either explicitly stated or set implicitly by the resolution of the technique used to digitize particle motions. Such criteria retain the important property of mass conservation as long as the mobile and immobile states encompass all grains and are mutually exclusive, and mobile particles are not counted towards the elevation of the bed. Moreover, velocity criteria are valid in scenarios where sediment transport and morphodynamics are dominated by bedload transport rather than granular creep.

Other criteria that are equally defensible from a theoretical perspective may lead to different results as to whether certain particles are mobile or immobile, ultimately producing differences in measured distributions of particle hop distance and travel time (HosseiniSadabadi et al., 2019). We recognize this issue but do not attempt to solve it here. Instead, we use an approach that is similar to previous studies (Liu et al., 2019) and acknowledge where our results might be sensitive to this choice. Velocity criteria are an objective, reproducible solution to this problem. Different velocity thresholds may produce different distributions of particle hop distance and travel time but will lead to essentially the same estimate of the macroscopic flux as long as the velocity threshold is sufficiently small.

The exact value of the velocity threshold used here was chosen following the approach of Liu et al. (2019). Specifically, we examined particle motions under a range of velocity thresholds and found that values ranging from 0.2 cm/s to 0.5 cm/s reliably discriminated between visually-identified mobile and immobile states. The exact value of the threshold within this range affects the absolute magnitude of empirical moments but has almost no effect on the primary findings of this paper which concern their relative magnitudes and the shape of the distribution functions. Reported results were obtained using a velocity threshold of 0.3 cm/s. This value is significantly lower than the threshold velocities adopted by Liu et al. (2019) and Lajeunesse et al. (2010), perhaps because the lower frame rate (30 frames per second in the present study compared with 90 frames per second) allows more precise estimates of frame-averaged velocity. This number corresponds to a one-frame displacement of 0.01 cm over $1/30^{th}$ of a second, which is roughly one pixel or one third of the median grain diameter. Particles with frame-averaged velocities greater than or equal to the threshold velocity are considered mobile, and all other particles are considered immobile. A complete hop is defined as an uninterrupted period in the mobile state that begins and ends with transitions to and from the immobile state. Insofar as previous plane-bed studies necessarily employ some variant of this approach, it is sufficient to reveal the extent to which particle motions over bedforms conform to existing theory.

4 Results and Discussion

The experimental procedure described in the previous section yielded measurements of 360 complete particle hops for the plane bed condition and 1170 hops for the bedform

Table 1. Summary Statistics

	Plane Bed	Bedforms
Mean travel time $\overline{T_p}$	0.18 s	0.13 s
Variance $\sigma^2_{T_p}$	0.042 s^2	0.023 s^2
Coefficient of variation $\sigma_{T_p}/\overline{T_p}$	1.13	1.13
Mean streamwise hop distance $\overline{L_x}$	0.32 cm	0.21 cm
Variance $\sigma^2_{L_x}$	0.43 cm^2	0.47 cm^2
Coefficient of variation $\sigma_{L_x}/\overline{L_x}$	2.04	3.25
Streamwise diffusion length ℓ_{D_x}	1.34 cm	2.22 cm
Inverse Peclet number Pe_x^{-1}	4.2	10.6
Mean lateral hop distance $\overline{L_y}$	-2.2 $\times$ 10^{-3} cm	-2.8$\times$ 10^{-2} cm
Variance $\sigma^2_{L_y}$	0.11 cm^2	0.27 cm^2
CV of absolute values $\sigma_{\lvert L_y\rvert}/\overline{\lvert L_y\rvert}$	2.20	2.70
Coefficient of lateral transport $\sigma_{L_y}/\overline{L_x}$	1.03	2.49
Lateral diffusion length ℓ_{D_y}	0.34 cm	1.29 cm
Inverse Peclet number Pe_y^{-1}	1.07	6.17

condition. These data are visualized in Figure 1, which shows all tracked particle motions, and Figure 2, which shows the pairwise relationships between variables. Descriptive statistics are reported in Table (1).

Tracked particle paths reveal significant qualitative differences between the plane-bed and bedform experiments. Notably, particle behavior clearly depends on position relative to bedform features in a manner that is reminiscent of the backward facing step experiments of Leary and Schmeeckle (2017) and the particle velocity fields reported by Tsubaki et al. (2018) and Terwisscha van Scheltinga et al. (2019). Particle transport direction is highly variable in the region of flow separation immediately downstream of the bedform crest. On the stoss side, particle transport direction is more regular and the mean local transport direction is approximately perpendicular to the nearest crest (Figure 1).

Empirical moments are reported in Table 1. Although the mean particle travel time and mean streamwise hop distance are slightly larger in the plane-bed experiment, we find that the distribution of particle hop distances over bedforms has much larger variance in the cross-stream and streamwise directions. The sample size in both experiments was sufficiently large such that conventional measures of statistical uncertainty indicate that moments are estimated with a unrealistically high precision. For example, the 95% asymptotic confidence interval for the estimate of the mean travel time in the bedform experiment ranges from 0.12 s to 0.14 s. More sophisticated estimates of statistical uncertainty produce similar results, however they do not capture unquantifiable uncertainty associated with imperfect experimental methodology. Due to the systematic misrepresentation of true uncertainty, confidence intervals for other parameters are not reported here.

4.1 Physical Mechanism for Observed Differences in Particle Behavior

Previous studies of particle motion find that particle velocities are conditionally dependent on the local topographic configuration due to the coupling of topography, flow, and sediment transport (Tsubaki et al., 2018; Terwisscha van Scheltinga et al., 2019). Topographically-induced correlations in flow velocity exist over spatial scales that are comparable to the bedform length; in contrast, we find that the average hop distance is much smaller than a bedform length. As a result, individual particle hops do not con-

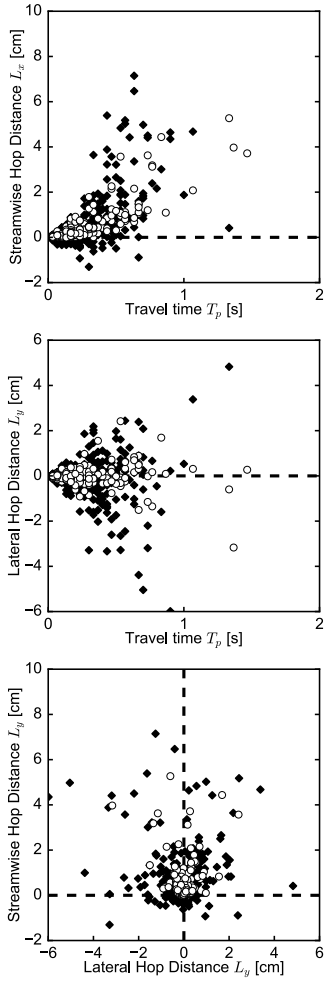

Figure 2. Pairwise comparison of measured particle hop distances and travel times. Dashed lines indicate particle hop distances of zero. Bedform data are shown in black diamonds and plane-bed data are shown in white circles.

verge on the ensemble statistics of motion (Fathel et al., 2016; Furbish et al., 2017), instead reflecting topographically-induced deviations from the mean flow field.

As an example, consider a particle that is entrained on a stoss slope that is oriented obliquely relative to the mean flow direction. This topographic configuration usually results in flow being redirected laterally (Best, 2005; Venditti et al., 2005b), causing a corresponding lateral component of sediment movement (Tsubaki et al., 2018; Terwisscha van Scheltinga et al., 2019) that is possibly amplified by gravitational effects (Parker et al., 2003). Because particle motions are short relative to the spatial scales of topography, this particle is likely to spend the entire interval from entrainment to disentrainment on this oblique slope. A large lateral hop distance would be highly improbable over plane-bed topography under similar mean flow conditions, but would be typical for particles entrained in this location.

We suggest that observed differences in probability distributions of particle hop distance and travel time are the result of this effect. Over plane-bed topography, turbulent fluctuations in flow velocity and collisions between particles are the primary sources of variability (Nikora et al., 2001, 2002; Seizilles et al., 2014; Fathel et al., 2015; Hossein-

iSadabadi et al., 2019). We infer that localized fluctuations in flow velocity driven by bedform topography cause variability in particle behavior that is superimposed on variability driven by turbulence and particle collisions. Tsubaki et al. (2018) and Terwisscha van Scheltinga et al. (2019) report similar behaviors, which manifest as deviations from the mean particle velocity field characterized by crest-normal transport on the stoss sides of bedforms (Fryberger & Dean, 1979; Werner & Kocurek, 1997), and highly variable transport over lee faces and troughs (figures 1c, 1d). This causes a marked difference in particle displacement behavior including an increase in the variability in particle hop distances (figures 1e, 1f). Quantitative analyses presented below contextualize these observations in terms of the entrainment forms of the flux and Exner equations.

4.2 Effect of Naturally-Sorted Sediment

Our analysis assumes that the marginal distributions of particle hop distance and travel time have thin tails such that the mean and the variance are well defined. Although previous studies suggest that this is true for monodisperse sediment undergoing low bedload transport (Fathel et al., 2015; Furbish et al., 2016; Liu et al., 2019), heavy-tailed distributions of hop distance and travel time are possible if a range of grain sizes are present and the mean hop distance varies with grain size (Ganti et al., 2010). Our experiments involved naturally-sorted sediment which is valuable insofar as we seek to understand natural transport systems. However, it is important to consider the extent to which theory developed for uniform sediment may be applicable to the present research.

As a starting point, we consider the distribution of streamwise hop distance as a margin of the joint distribution of particle hop distance and grain size, $f_{L_x,D}(L_x, D)$:

$$f_{L_x}(L_x) = \int_0^\infty f_{L_x|D}(L_x|D) f_D(D) dD. \tag{6}$$

Ganti et al. (2010) clarify how this integration may lead to a heavy-tailed distribution of hop distance. Specifically, if $f_{L_X|D}(L_x|D)$ is exponential with mean varying in proportion (or inverse proportion) to grain size and $f_D(D)$ is a Gamma distribution with shape parameter α, then $f_{L_x}(L_x)$ is a generalized Pareto distribution. This argument also holds for particle travel times. In this scenario, the mean only converges if $\alpha > 1$ and the variance only converges if $\alpha > 2$. We note that the the coefficient of variation of a Gamma distribution is equal to $1/\sqrt{\alpha}$. Thus, the weight of the tails depends on the degree of sorting of the bed material, where well-sorted sediments are less likely to have heavy-tailed distributions of hop distance and travel time. The best-fit Gamma distribution for the bed material used in these experiments has a shape parameter $\alpha = 4.83$ such the mean and variance are well-defined. On this basis, we suggest that it is reasonable to expect that the distributions of hop distance and travel time are thin-tailed. Furthermore, this may be a universal outcome of mature hydraulic sorting.

Even if the distributions have thin tails, variability in grain size implies that the marginal probability distributions of hop distance and travel time depend on (a) the functional form of the grain-size specific distribution of hop distance and travel time (e.g. $f_{L_x|D}(L_x|D)$, (b) the relationship between the grain size and the parameters of this conditional distribution, and (c) the relative entrainment rates of different grain sizes (which may differ from the grain size distribution of the bed material due to selective entrainment and vertical sorting). Each of these effects may be present in our data, however we focus on the collective outcome and have not attempted to evaluate their importance individually.

4.3 Comparison of Theoretical and Empirical Distributions

4.3.1 Travel Times

Previous studies suggest that the marginal probability distribution of bedload particle travel times is exponential (Fathel et al., 2015; Furbish et al., 2016), i.e.:

$$f_{T_p}(T_p) = \frac{1}{\tau} e^{-T_p/\tau}, \tag{7}$$

where τ is a characteristic travel time. This implies a fixed temporal disentrainment rate for moving particles (Furbish et al., 2016). In other words, the probability that a particle in motion at time t is deposited over the next small time interval dt does not depend on how long the particle has been in motion at t.

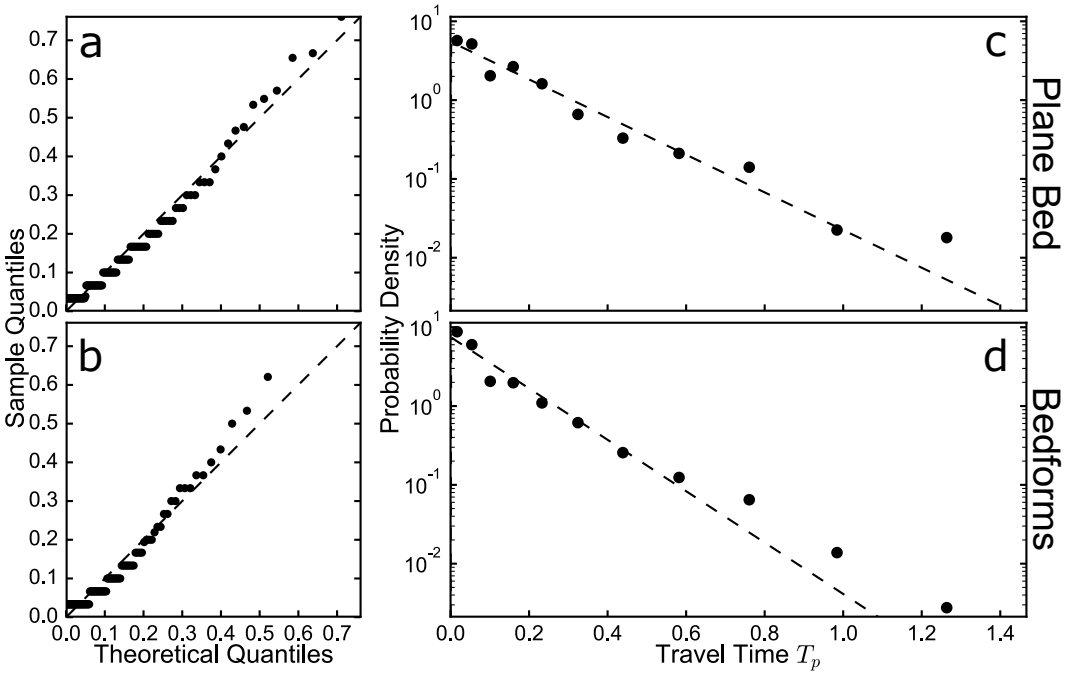

Figure 3. Quantile-quantile (a, b) and density plots (c,d) comparing measured distributions of particle travel time with best-fit exponential distributions (dashed lines). Densities were computed using logarithmically-spaced bins.

Quantile-quantile (Q-Q) plots (figure 3a, 3b) and histograms (figure 3c, 3d) reveal that the exponential distribution provides a good fit to plane-bed and bedform particle travel times (Figure 3). The coefficient of variation (the ratio of the standard deviation to the mean) of an exponentially distributed random variable is 1, which is an important diagnostic test of distribution fit. Measured coefficients of variation are 1.13 for both experiments (Table 1). Based on these observations, we suggest that (a) our data confirm the findings of previous authors with regard to the exponential distribution of particle travel times over plane-bed topography and (b) the presence of equilibrium mobile bedforms does not substantially influence the functional form of this distribution. We also find no evidence that the distribution of travel times is heavy-tailed despite variability in bed material grain size typical of natural fluvial systems.

4.3.2 Streamwise Hop Distances

Theoretical distributions proposed by Fathel et al. (2015) to describe streamwise hop distances follow from exponentially distributed travel times combined with the assumption that particles with longer travel times have the opportunity to attain higher velocities (Roseberry et al., 2012). This suggests that a conditional dependence of particle hop distance on travel time that can be approximated by $L_x = a_x T_p^{b_x} + \epsilon_x$ (Fathel et al., 2015), where a_x is a characteristic acceleration, ϵ_x is a residual deviation term, and b_x is a scaling parameter that may be connected to suspension conditions. For bedload-dominated transport, particle travel times are short relative to the timescale required to accelerate particles to the mean near-bed fluid velocity and particle hops are dominated by the unsteady acceleration and deceleration phases of motion (Campagnol et al., 2015). As a result, previous studies which report bedload-dominated transport over plane-bed topography (e.g., Fathel et al., 2015) find that $L_x/T_p \sim T_p$ and leading to $b_x = 2$. It has been suggested that this dependence disappears at higher suspension conditions (Ancey & Heyman, 2014; Heyman et al., 2016; Campagnol et al., 2015; Wu et al., 2020), however we restrict our attention to bedload-dominated transport similar to previous plane-bed studies. Ignoring the residual deviation and assuming exponentially distributed travel times leads to the expectation that hop distances follow Weibull distributions (Fathel et al., 2015). Thus, the marginal distribution of streamwise hop distances is given by

$$f_{L_x}(L_x) = \frac{k_x}{\lambda_x}\left(\frac{x}{\lambda_x}\right)^{k_x - 1} e^{-(x/\lambda)^{k_x}} \tag{8}$$

where $k_x = 1/b_x$ and $\lambda_x = a_x \tau^{b_x}$. If $k_x = 1/2$, then the mean and variance in particle hop distance can be expressed in terms of model parameters as $\overline{L_x} = 2a_x\tau^2$ and $\sigma^2_{L_x} = 20a_x^2\tau^4$.

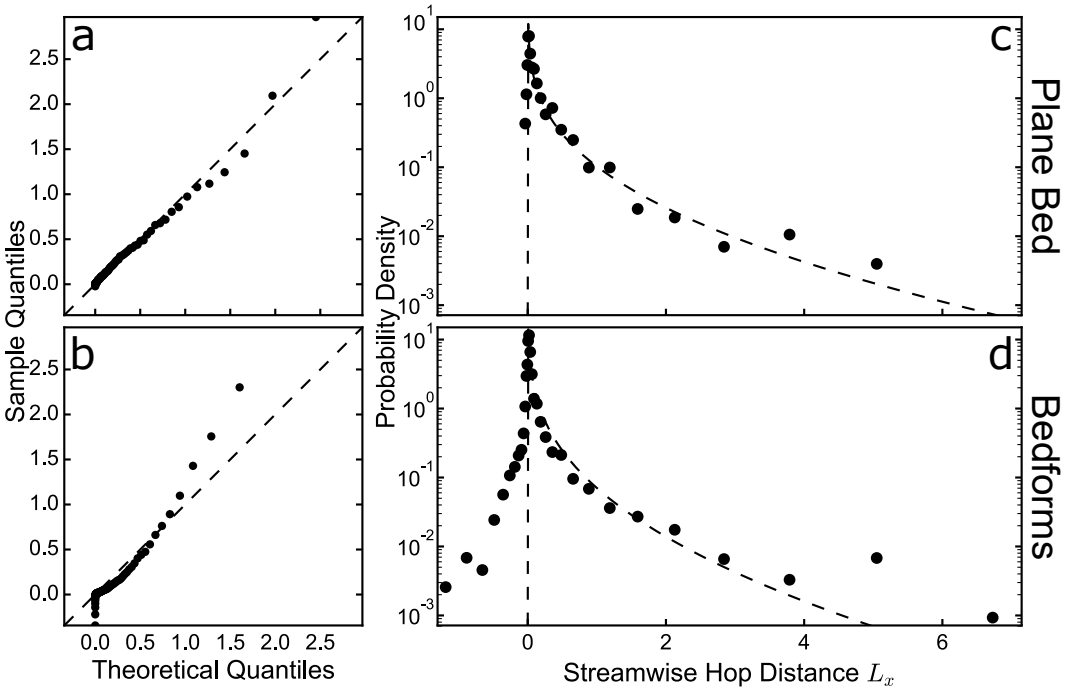

Figure 4. Quantile-quantile (a, b) and density plots (c, d) comparing measured distributions of streamwise hop distance with best-fit Weibull distributions with shape parameter $k = 1/2$ (dashed lines). Densities were computed using logarithmically-spaced bins.

In considering whether this distribution is suitable for hop distances over bedforms, we focus primarily on the considerations relevant to macroscopic morphodynamic modeling outlined in Section 2. Specifically, we ask whether estimates of distribution parameters a_x and τ can lead to accurate predictions of the mean hop distance $\overline{L_x}$ and the variance $\sigma^2_{L_x}$. This question is of central importance if the eventual goal is to construct macroscopic morphodynamic models that are consistent with the physics of grain-scale sediment transport. The proposed Weibull distribution with shape parameter $k = 1/2$ prescribes a fixed coefficient of variation $\sqrt{5} \approx 2.23$. This implies that the variance $\sigma^2_{L_x}$ can be estimated from a measurement of the mean. If k is allowed to vary between $1/2$ and 1, the coefficient of variation must be between 1 and $\sqrt{5}$. The coefficient of variation therefore is an important indicator of distribution fit; if it is significantly larger than $\sqrt{5}$ or smaller than 1, no single estimate of model parameters appropriately characterizes the advective and diffusive components of the flux simultaneously.

Measured streamwise hop distances in the plane-bed experiment have a coefficient of variation of 2.05 compared with 2.23 predicted from theory. Ignoring upstream hops does not significantly affect the estimate of the mean because only 5% of hops occur in the upstream direction and the average upstream hop distance is very small relative to the average downstream hop distance (0.1 mm compared with 3.5 mm). As with travel times, we find no evidence that the distribution of particle hop distance is heavy-tailed for the moderately-sorted sand used in this experiment. We suggest suggest that the distribution of streamwise bedload hop distances over plane-bed topography in hydraulically-sorted, natural sediments can be sufficiently approximated using a Weibull distribution with shape parameter $k = 1/2$ in the context of macroscopic transport problems.

In contrast, the the distribution of streamwise hop distances over bedforms exhibits significant deviations from theory. Qualitative comparison of the histogram and a best-fit theoretical distribution (figure 4d) reveals systematic differences in probability density across the full range of observed hop distances that results in a concave-up relationship between empirical and theoretical quantiles (Figure 4b). A much larger fraction of hops occur in the upstream direction (15%) and these possess an average upstream displacement that are a significant fraction of the average downstream displacement (0.8 mm compared with 2.8 mm). We conclude that the presence of bedforms leads to an important difference in empirical moments: the coefficient of variation in measured streamwise hop distances is 3.25, meaning that the standard deviation does not vary with the mean as expected. Instead, observed spatiotemporal correlations between particle behavior and topography lead to an increased variance relative to the mean (figure 1d, 1f) that violates constraints imposed by plane-bed theory.

4.3.3 Lateral Hop Distances

The streamwise and lateral coordinates are defined such that lateral hop distances have a mean of zero and are symmetrically distributed under steady, uniform transport conditions considered here. Like with streamwise hop distances, Roseberry et al. (2012) and Fathel et al. (2015) find that the absolute lateral displacement is correlated with travel time leading to $|L_y| = a_y T_p^{b_y} + \epsilon_y$, where $b_y \approx 2$. The distribution of absolute lateral hop distances can therefore be approximated using a Weibull distribution with shape parameter $k = 1/2$ and scale parameter $\lambda = a_y\tau^2$. The mean absolute lateral hop distance is given by $\overline{|L_y|} = 2a_y\tau^2$, the variance is given by $\sigma^2_{|L_y|} = 20a_y^2\tau^4$, and the coefficient of variation is $\sqrt{5}$. Because the distribution of signed lateral hop distances is symmetric with mean equal to zero, the variance is equal to the raw variance of absolute lateral hop distances, i.e. $\sigma^2_{L_y} = \overline{|L_y|^2} = \overline{|L_y|}^2 + \sigma^2_{|L_y|}$. The first and second moments that are relevant to macroscopic transport problems can be expressed in terms of distribution parameters as $\overline{L_y} = 0$ and $\sigma^2_{L_y} = 24a_y^2\tau^4$.

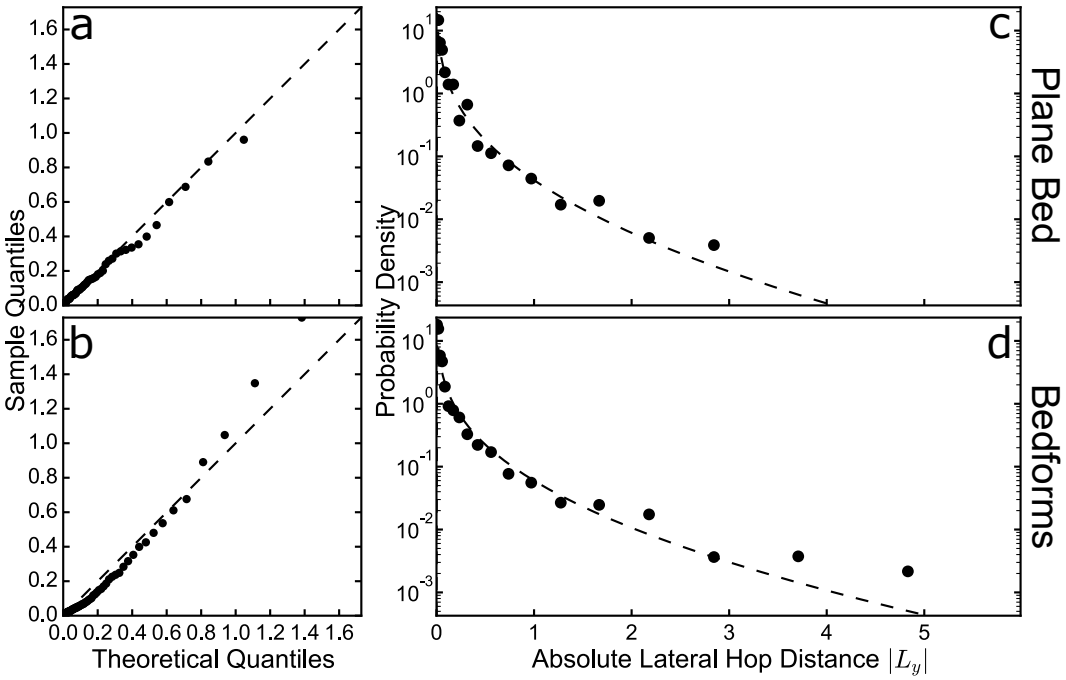

Figure 5. Quantile-quantile (a, b) and density plots (c, d) comparing measured distributions of absolute lateral hop distance with best-fit Weibull distributions with shape parameter $k = 1/2$ (dashed lines). Densities were computed using logarithmically-spaced bins.

The quantile-quantile plot (figure 5a) and histogram (figure 5c) reveal that absolute lateral hop distances over plane-bed topography are well-approximated by the best-fit Weibull distribution with fixed shape parameter $k = 1/2$. The empirical coefficient of variation for absolute lateral hop distances is 2.20, compared with 2.23 predicted from theory. For particle motions over bedform topography, the coefficient of variation in absolute lateral hop distances is 2.7, while the histogram plot (figure 5d) reveals systematic deviations from predicted bin frequencies resulting in a concave-up relationship between theoretical and measured quantiles (figure 5b). Again, this may indicate a heavy-tailed distribution of absolute lateral hop distances. If the distribution is not heavy tailed, then bedforms cause a significant increase in the variance of the signed lateral hop distances (0.27 cm^2 compared with 0.11 cm^2), both by altering the shape of the distribution of absolute lateral hop distances and by increasing the average absolute lateral hop distance. This result primarily reflects an increase in the variability in transport direction as characterized by the coefficient of lateral transport (Table 1).

4.4 Bedload Diffusion

We have found that bedforms increase the variance of the ensemble probability distributions of streamwise and absolute lateral hop distances. Here, we consider the significance of this observation in the context of macroscopic transport equations under the assumption that these moments are in fact finite and well-represented by our data. As noted previously, the Fokker-Planck approximation of the one dimensional entrainment flux consists of three terms: a local advective term that represents the mean hop distance, a nonlocal advective term that squared the squared mean, and a diffusive term that represents the variance. These three terms are not guaranteed to map directly onto the typical advective and diffusive terms contained in the activity form of the flux (Furbish et

al., 2012, 2017), thus we refer to the sum of the first two terms as the advective-like flux and the third term as a diffusive-like flux.

Nonlocal advective-like and diffusive-like transport terms are zero under steady, uniform transport conditions (Furbish et al., 2012). In order to compare the advective and diffusive behavior associated with a fixed distribution of particle hop distances, we consider a simple disequilibrium scenario in which the sediment flux varies due to a constant spatial gradient in the particle entrainment rate, $\partial E/\partial x = \beta$. In this case, the total flux is steady, varying only as a function of x and is given by:

$$q_x(x) = E(x)\overline{L_x} - \frac{1}{2}\beta\overline{L_x}^2 - \frac{1}{2}\beta\sigma_{L_x}^2. \tag{9}$$

and the flux gradient is given by

$$\frac{\partial}{\partial x}q_x(x) = \beta\overline{L_x} \tag{10}$$

The diffusive flux is related to gradients in the advective flux by a diffusion length ℓ_{D_x} (Seizilles et al., 2014) as

$$q_{x_{\text{diffusive}}} = -\ell_{D_x}\frac{\partial}{\partial x}q_x(x). \tag{11}$$

For the simple disequilibrium conditions considered here, this diffusion length reduces to $\ell_{D_x} = \sigma_{L_x}^2/\overline{L_x}$.

If hop distances are assumed to follow a Weibull distribution with shape parameter $k = 1/2$, the diffusion length is given by $\ell_{D_x} = 5\overline{L_x}$. The ratio of diffusion length to hop length $\ell_{D_x}/\overline{L_x}$ is like an inverse Peclet number in that it scales the relative propensity for diffusion-like and advection-like transport in the presence of gradients in particle entrainment rate. We recognize that the entrainment rate and the probability distributions of particle hop distance vary together in response to changes in boundary conditions; however, this mathematical abstraction is useful in that it enables a direct characterization of the effects of bedform development on particle diffusion.

For the plane bed experiment reported here, we find that measured distributions of particle hop distance lead to $\ell_{D_x} = 4.2\overline{L_x}$. Thus, the Weibull distribution proposed by previous authors appropriately predicts the measured relationship between streamwise diffusion and streamwise advection for naturally-sorted sediments transported over planar topography. In contrast, we find for the bedform condition that $\ell_{D_x} = 10.6\overline{L_x}$, deviating significantly from theory.

Following similar arguments presented above but assuming a constant lateral gradient in particle entrainment rate $\partial E/\partial y$, it is straightforward to show that the lateral diffusive flux is related to the lateral gradient in the streamwise advective flux by a diffusion length $\ell_{D_y} = \sigma_{L_y}^2/\overline{L_x}$. Though, we lack a clear basis for predicting the lateral diffusion length as we have done for the streamwise diffusion length above, we assume as a starting point that the lateral Peclet number is fixed over plane-bed topography (as theory predicts for the streamwise Peclet number). For measured particle hop distances over plane-bed topography, we find that $\ell_{D_y} = 1.07\overline{L_x}$. In contrast, particle motions in the bedform experiment have a lateral diffusion length of $\ell_{D_y} = 6.17\overline{L_x}$.

In summary, bedform development appears to increase the propensity for streamwise and lateral diffusive transport quantified by an inverse Peclet number that is equal to the squared coefficient of variation (for streamwise diffusion) or the squared coefficient of lateral transport (for lateral diffusion). This difference cannot be explained by an increase in shear stress alone which would likely cause an increase in the mean streamwise hop distance (Lajeunesse et al., 2010). Instead, bedform development results in a decrease of the mean streamwise hop distance with a concurrent increase of the variance of streamwise and lateral hop distances in our experiments. The notion that this difference is primarily caused by the development of bedform topography is entirely consistent with previously observed differences in particle behavior described by Wilson and Hay (2016),

Leary and Schmeeckle (2017), Tsubaki et al. (2018), and Terwisscha van Scheltinga et al. (2019).

4.5 Experimental Censorship

We have interpreted these data as representative of the ensemble distribution of particle hop distances and travel times characteristic of macroscopic flow conditions. In principle, this requires an unbiased sample of particle motions representing all possible microconfigurations of flow, topogrpahy, and sediment transport. However, practical considerations limited the spatiotemporal extent over which it was possible to measure particle motions. This has two effects which could potentially influence our results.

The first effect is related to the fact that particles with longer hop distances and travel times are more likely to begin or end their motions outside of the measurement window. This effect causes a systematic reduction in the sample mean and variance relative to the true mean and variance because hops are censored at a rate that is proportional to their duration and length. In order to evaluate the importance of this effect, we performed the correction proposed by Ballio et al. (2019). This correction resulted in almost no change in estimates of the mean or variance in either of our experiments. Although this correction cannot account for all forms of censorship (for example, truncation of the distribution), we are confident that our results are not substantially influenced by this effect.

The second effect concerns the fact that our sampling window is not large enough to capture a representative sample of particle motions originating from all possible microconfigurations of flow and topography characteristic of the macroscopic transport conditions. The importance of this effect cannot be evaluated directly from available data. Nevertheless, we argue that our data are sufficient to provide unequivocal support for the primary claims made in this paper. Observed differences in particle behavior are consistent with previous studies of particle motion over bedforms (e.g., Wilson & Hay, 2016; Leary & Schmeeckle, 2017; Tsubaki et al., 2018) and qualitative differences illustrated in figure 1. Additionally, the mean lateral hop distance in the bedform experiment is approximately zero (-0.028 cm) despite clear spatial correlations in lateral hop distance within the measurement window (Figure 1). Assuming the true mean lateral hop distance is zero, we tentatively interpret this as an indicator that the spatiotemporal extent of our measurement window is sufficiently large such that the measured statistics have begun to converge on the true ensemble statistics. By way of analogy, consider the problem of estimating the mean and variance of bed elevation in a stable bedform field. Measurements from a single bedform will provide reasonable first-order estimates of these quantities despite the fact that there is variability between bedforms (Robert & Richards, 1988; Nikora et al., 1997).

We argue that the primary findings of this paper concerning the forms of the distributions of particle hop distance and travel time over bedforms are robust to possible censorship effects. Increases in streamwise and lateral diffusivity are consistent with observations of particle motion reported by previous authors cannot be explained by censorship or sampling biases.

5 Conclusions

This paper presents results of an experimental study comparing the probability distributions that describe the spatiotemporal scales of particle motion linking particle entrainment and disentrainment events. Measured distributions of particle travel time, T_p, streamwise hop distance, L_x, and lateral hop distance, L_y, are compared with previously proposed theoretical distributions describing particle motions over plane-bed topography. We confirm that particle motions over plane-bed topography in natural sediments

conform to existing theory. Travel times follow an exponential distribution while streamwise and absolute lateral hop distances follow a Weibull distribution with shape parameter $k = 1/2$.

In contrast, we find that particle hop distances over bedforms possess an increased standard deviation in both the streamwise and lateral directions relative to the mean streamwise hop distance. We argue that this effect is consistent with observations of particle motion over bedforms reported by previous authors; Eulerian quantities like particle activity and velocity vary systematically in relation to topographic position. Topographically-induced deviations from mean-particle behavior are coupled with local flow velocity resulting in an additional source of variability that is superimposed on turbulent flow and particle collision effects. At the macroscopic scale, this means that the relative magnitudes of advective and diffusive-like transport implied by plane-bed distributions cannot be assumed when bedforms are present. Instead, bedforms increase the propensity for streamwise and lateral diffusion-like transport.

Acknowledgments

We thank the donors of the American Chemical Society Petroleum Research Fund 54492-DNI8, the National Science Foundation (NSF) grant EAR-1632938, and the University of Wyoming School for Energy Resources for partially supporting this research. Data supporting the analysis and conclusions presented here are available in the supporting information and through Figshare (Ashley et al., 2019).

References

Abbott, J. E., & Francis, J. R. D. (1977). Saltation and suspension trajectories of solid grains in a water stream. *Philosophical Transactions of the Royal Society of London. Series A, Mathematical and Physical Sciences*, *284*(1321), 225–254. doi: 10.1098/rsta.1977.0009

Abramian, A., Devauchelle, O., Seizilles, G., & Lajeunesse, E. (2019). Boltzmann Distribution of Sediment Transport. *Physical Review Letters*, *123*(1), 014501. doi: 10.1103/PhysRevLett.123.014501

Ancey, C. (2010). Stochastic modeling in sediment dynamics: Exner equation for planar bed incipient bed load transport conditions. *Journal of Geophysical Research: Earth Surface*, *115*(F2), 1–21. doi: 10.1029/2009JF001260

Ancey, C., & Heyman, J. (2014). A microstructural approach to bed load transport: mean behaviour and fluctuations of particle transport rates. *Journal of Fluid Mechanics*, *744*, 129–168. doi: 10.1017/jfm.2014.74

Ashley, T., Mahon, R., Naqshband, S., Leary, K., & McElroy, B. (2019). *Particle motions over plane-bed and bedform topography.* Figshare Dataset. doi: 10.6084/m9.figshare.11413038.v2

Bagherimiyab, F., & Lemmin, U. (2013). Shear velocity estimates in rough-bed open-channel flow. *Earth Surface Processes and Landforms*, *38*(14), 1714–1724. doi: 10.1002/esp.3421

Ballio, F., Pokrajac, D., Radice, A., & Hosseini Sadabadi, S. A. (2018). Lagrangian and Eulerian Description of Bed Load Transport. *Journal of Geophysical Research: Earth Surface*, *123*(2), 384–408. doi: 10.1002/2016JF004087

Ballio, F., Radice, A., Fathel, S. L., & Furbish, D. J. (2019). Experimental Censorship of Bed Load Particle Motions and Bias Correction of the Associated Frequency Distributions. *Journal of Geophysical Research: Earth Surface*, *124*(1), 116–136. doi: 10.1029/2018JF004710

Best, J. L. (1992). On the entrainment of sediment and initiation of bed defects: insights from recent developments within turbulent boundary layer research. *Sedimentology*, *39*(5), 797–811. doi: 10.1111/j.1365-3091.1992.tb02154.x

Best, J. L. (2005). The fluid dynamics of river dunes: A review and some future

research directions. *Journal of Geophysical Research: Earth Surface*, *110*(F4). doi: 10.1029/2004JF000218

Best, J. L. (2009). Kinematics, Topology and Significance of Dune-Related Macroturbulence: Some Observations from the Laboratory and Field. *Fluvial Sedimentology VII*, 41–60. doi: 10.1002/9781444304350.ch3

Bradski, G. (2000). The OpenCV Library. *Dr. Dobb's Journal of Software Tools*, *25*.

Campagnol, J., Radice, A., Ballio, F., & Nikora, V. (2015). Particle motion and diffusion at weak bed load: accounting for unsteadiness effects of entrainment and disentrainment. *Journal of Hydraulic Research*, *53*(5), 633–648. doi: 10.1080/00221686.2015.1085920

Charru, F., Andreotti, B., & Claudin, P. (2013). Sand Ripples and Dunes. *Annual Review of Fluid Mechanics*, *45*(1), 469–493. doi: 10.1146/annurev-fluid-011212-140806

Coleman, S. E., & Nikora, V. I. (2011). Fluvial dunes: Initiation, characterization, flow structure. *Earth Surface Processes and Landforms*, *36*(1), 39–57. doi: 10.1002/esp.2096

Coleman, S. E., Nikora, V. I., McLean, S. R., Clunie, T. M., Schlicke, T., & Melville, B. W. (2006). Equilibrium hydrodynamics concept for developing dunes. *Physics of Fluids*, *18*(10). doi: 10.1063/1.2358332

Costello, W. R. (1974). *Development of bed configurations in coarse sands* (Ph. D. Thesis). Massachusetts Institute of Technology.

Fathel, S., Furbish, D., & Schmeeckle, M. (2016). Parsing anomalous versus normal diffusive behavior of bedload sediment particles. *Earth Surface Processes and Landforms*, *41*(12), 1797–1803. doi: 10.1002/esp.3994

Fathel, S., Furbish, D. J., & Schmeeckle, M. W. (2015). Experimental evidence of statistical ensemble behavior in bed load sediment transport. *Journal of Geophysical Research: Earth Surface*, *120*(11), 2298–2317. doi: 10.1002/2015JF003552

Fryberger, S. G., & Dean, G. (1979). Dune Forms and Wind Regime. *USGS Professional Paper 1052*, 137–170.

Furbish, D. J., Fathel, S. L., Schmeeckle, M. W., Jerolmack, D. J., & Schumer, R. (2017). The elements and richness of particle diffusion during sediment transport at small timescales. *Earth Surface Processes and Landforms*, *42*(1), 214–237. doi: 10.1002/esp.4084

Furbish, D. J., Haff, P. K., Roseberry, J. C., & Schmeeckle, M. W. (2012). A probabilistic description of the bed load sediment flux: 1. Theory. *Journal of Geophysical Research: Earth Surface*, *117*(F3). doi: 10.1029/2012JF002352

Furbish, D. J., & Schmeeckle, M. W. (2013). A probabilistic derivation of the exponential-like distribution of bed load particle velocities. *Water Resources Research*, *49*(3), 1537–1551. doi: 10.1002/wrcr.20074

Furbish, D. J., Schmeeckle, M. W., Schumer, R., & Fathel, S. L. (2016). Probability distributions of bed load particle velocities, accelerations, hop distances, and travel times informed by Jaynes's principle of maximum entropy. *Journal of Geophysical Research: Earth Surface*, *121*(7), 1373–1390. doi: 10.1002/2016JF003833

Ganti, V., Meerschaert, M. M., Foufoula-Georgiou, E., Viparelli, E., & Parker, G. (2010). Normal and anomalous diffusion of gravel tracer particles in rivers. *Journal of Geophysical Research: Earth Surface*, *115*(F2), 1–12. doi: 10.1029/2008JF001222

García, M. H. (2008). Chapter 2: Sediment Transport and Morphodynamics. In *Sedimentation engineering: Process, management, modeling and practice* (pp. 21–164). American Society of Civil Engineers.

Gibbs, J. W. (1902). *Elementary Principles in Statistical Mechanics*. New Haven: Yale University Press.

Heyman, J., Bohorquez, P., & Ancey, C. (2016). Entrainment, motion, and deposition of coarse particles transported by water over a sloping mobile bed. *Journal of Geophysical Research: Earth Surface*, *121*(10), 1931–1952. doi: 10.1002/2015JF003672

HosseiniSadabadi, S. A., Radice, A., & Ballio, F. (2019). On Reasons of the Scatter of Literature Data for BedLoad Particle Hops. *Water Resources Research*, *55*(2), 1698–1706. doi: 10.1029/2018WR023350

Houssais, M., & Jerolmack, D. J. (2017). Toward a unifying constitutive relation for sediment transport across environments. *Geomorphology*, *277*, 251–264. doi: 10.1016/j.geomorph.2016.03.026

Houssais, M., Ortiz, C. P., Durian, D. J., & Jerolmack, D. J. (2015). Onset of sediment transport is a continuous transition driven by fluid shear and granular creep. *Nature Communications*, *6*(1), 6527. doi: 10.1038/ncomms7527

Kwoll, E., Venditti, J. G., Bradley, R. W., & Winter, C. (2017). Observations of Coherent Flow Structures Over Subaqueous High- and Low- Angle Dunes. *Journal of Geophysical Research: Earth Surface*, *122*(11), 2244–2268. doi: 10.1002/2017JF004356

Lajeunesse, E., Malverti, L., & Charru, F. (2010). Bed load transport in turbulent flow at the grain scale: Experiments and modeling. *Journal of Geophysical Research: Earth Surface*, *115*(4). doi: 10.1029/2009JF001628

Le Bouteiller, C., & Venditti, J. G. (2015). Sediment transport and shear stress partitioning in a vegetated flow. *Water Resources Research*, *51*(4), 2901–2922. doi: 10.1002/2014WR015825

Leary, K. C. P., & Schmeeckle, M. W. (2017). The Importance of Splat Events to the Spatiotemporal Structure of Near-Bed Fluid Velocity and Bedload Motion over Bedforms: Laboratory Experiments Downstream of a Backward-Facing Step. *Journal of Geophysical Research: Earth Surface*. doi: 10.1002/2016JF004072

Liu, M. X., Pelosi, A., & Guala, M. (2019). A Statistical Description of Particle Motion and Rest Regimes in OpenChannel Flows Under Low Bedload Transport. *Journal of Geophysical Research: Earth Surface*, *124*(11), 2666–2688. doi: 10.1029/2019JF005140

Maddux, T. B., McLean, S. R., & Nelson, J. M. (2003). Turbulent flow over three-dimensional dunes: 2. Fluid and bed stresses. *Journal of Geophysical Research: Earth Surface*, *108*(F1), n/a–n/a. Retrieved from `http://doi.wiley.com/10.1029/2003JF000018` doi: 10.1029/2003JF000018

Maddux, T. B., Nelson, J. M., & McLean, S. R. (2003). Turbulent flow over three-dimensional dunes: 1. Free surface and flow response. *Journal of Geophysical Research: Earth Surface*, *108*(F1), n/a–n/a. Retrieved from `http://doi.wiley.com/10.1029/2003JF000017` doi: 10.1029/2003JF000017

McElroy, B. (2009). *Expressions and Implications of Sediment Transport Variability in Sandy Rivers* (Ph.D. Dissertation). University of Texas, Austin.

McLean, S. R. (1990). The stability of ripples and dunes. *Earth-Science Reviews*, *29*(1-4), 131–144. doi: 10.1016/0012-8252(0)90032-Q

Mclean, S. R., Nelson, J. M., & Wolfe, S. R. (1994). Turbulence structure over two-dimensional bed forms: Implications for sediment transport. *Journal of Geophysical Research*, *99*(C6), 12729–12747. doi: 10.1029/94JC00571

Muste, M., Baranya, S., Tsubaki, R., Kim, D., Ho, H., Tsai, H., & Law, D. (2016). Acoustic mapping velocimetry. *Water Resources Research*, *52*(5), 4132–4150. doi: 10.1002/2015WR018354

Naqshband, S., McElroy, B., & Mahon, R. C. (2017). Validating a universal model of particle transport lengths with laboratory measurements of suspended grain motions. *Water Resources Research*, *53*(5), 4106–4123. doi: 10.1002/2016WR020024

Nikora, V., Habersack, H., Huber, T., & McEwan, I. (2002). On bed particle dif-

fusion in gravel bed flows under weak bed load transport. *Water Resources Research*, *38*(6). doi: 10.1029/2001WR000513

Nikora, V., Heald, J., Goring, D., & McEwan, I. (2001). Diffusion of saltating particles in unidirectional water flow over a rough granular bed. *Journal of Physics A: Mathematical and General*, *34*(50), L743–L749. doi: 10.1088/0305-4470/34/50/103

Nikora, V., Sukhodolov, A., & Rowinski, P. (1997). Statistical sand wave dynamics in one-directional water flows. *Journal of Fluid Mechanics*, *351*, 17–39. doi: 10.1017/s0022112097006708

Nordin, C. F. (1971). *Statistical properties of dune profiles* (Vol. 562).

Parker, G., Paola, C., & Leclair, S. (2000). Probabilistic Exner Sediment Continuity Equation for Mixtures with No Active Layer. *Journal of Hydraulic Engineering*, *126*(11), 818–826. doi: 10.1061/(ASCE)0733-9429(2000)126:11(818)

Parker, G., Seminara, G., & Solari, L. (2003). Bed load at low Shields stress on arbitrarily sloping beds: Alternative entrainment formulation. *Water Resources Research*, *39*(7), 1–11. doi: 10.1029/2001WR001253

Pelosi, A., & Parker, G. (2014). Morphodynamics of river bed variation with variable bedload step length. *Earth Surface Dynamics*, *2*(1), 243–253. doi: 10.5194/esurf-2-243-2014

Robert, A., & Richards, K. S. (1988). On the modelling of sand bedforms using the semivariogram. *Earth Surface Processes and Landforms*, *13*(5), 459–473. doi: 10.1002/esp.3290130510

Roseberry, J. C., Schmeeckle, M. W., & Furbish, D. J. (2012). A probabilistic description of the bed load sediment flux: 2. Particle activity and motions. *Journal of Geophysical Research: Earth Surface*, *117*(F3). doi: 10.1029/2012JF002353

Rueden, C. T., Schindelin, J., Hiner, M. C., DeZonia, B. E., Walter, A. E., Arena, E. T., & Eliceiri, K. W. (2017). ImageJ2: ImageJ for the next generation of scientific image data. *BMC Bioinformatics*, *18*(1), 529. doi: 10.1186/s12859-017-1934-z

Schindelin, J., Arganda-Carreras, I., Frise, E., Kaynig, V., Longair, M., Pietzsch, T., ... Cardona, A. (2012). Fiji: an open-source platform for biological-image analysis. *Nature Methods*, *9*(7), 676–682. doi: 10.1038/nmeth.2019

Seizilles, G., Lajeunesse, E., Devauchelle, O., & Bak, M. (2014). Cross-stream diffusion in bedload transport. *Physics of Fluids*, *26*(1), 013302. doi: 10.1063/1.4861001

Simons, D. B., Richardson, E. V., & Nordin, C. F. (1965). Bedload equation for ripples and dunes. *Sediment Transport in Alluvial Channels, Geological Survey Professional Paper 462-H*, 1–9.

Southard, J. B., & Boguchwal, L. A. (1990). Bed configurations in steady unidirectional water flows. Part 2. Synthesis of flume data. *Journal of Sedimentary Petrology*, *60*(5), 658–679. doi: 10.1306/212f9241-2b24-11d7-8648000102c1865d

Southard, J. B., & Dingler, J. R. (1971). Flume Study of Ripple Propagation Behind Mounds on Flat Sand Beds. *Sedimentology*, *16*(3-4), 251–263. doi: 10.1111/j.1365-3091.1971.tb00230.x

Terwisscha van Scheltinga, R. C., Coco, G., & Friedrich, H. (2019). Sand particle velocities over a subaqueous dune slope using highfrequency image capturing. *Earth Surface Processes and Landforms*, *44*(10), 1881–1894. doi: 10.1002/esp.4617

Tinevez, J.-Y., Perry, N., Schindelin, J., Hoopes, G. M., Reynolds, G. D., Laplantine, E., ... Eliceiri, K. W. (2017). TrackMate: An open and extensible platform for single-particle tracking. *Methods*, *115*, 80–90. doi: 10.1016/j.ymeth.2016.09.016

Tsubaki, R., Baranya, S., Muste, M., & Toda, Y. (2018). Spatio-temporal patterns

of sediment particle movement on 2D and 3D bedforms. *Experiments in Fluids*, *59*(6), 93. doi: 10.1007/s00348-018-2551-y

Tsujimoto, T. (1978). *Probabilistic model of the process of bed load transport and its application to mobile-bed problems* (Ph.D. Dissertation). Kyoto University, Kyoto, Japan.

Van Den Berg, J. H., & Van Gelder, A. (1993). A New Bedform Stability Diagram, with Emphasis on the Transition of Ripples to Plane Bed in Flows over Fine Sand and Silt. In *Alluvial sedimentation* (pp. 11–21). Oxford, UK: Blackwell Publishing Ltd. doi: 10.1002/9781444303995.ch2

Van Der Mark, C. F., & Blom, A. (2007). A new & widely applicable bedform tracking tool. *Enschede, The Netherlands. University of Twente*, *31*.

Venditti, J. G., Church, M., & Bennett, S. J. (2005b). On the transition between 2D and 3D dunes. *Sedimentology*, *52*(6), 1343–1359. doi: 10.1111/j.1365-3091.2005.00748.x

Venditti, J. G., Church, M., & Bennett, S. J. (2006). On interfacial instability as a cause of transverse subcritical bed forms. *Water Resources Research*, *42*(7), 1–10. doi: 10.1029/2005WR004346

Venditti, J. G., Church, M. A., & Bennett, S. J. (2005a). Bed form initiation from a flat sand bed. *Journal of Geophysical Research: Earth Surface*, *110*(1), 1–19. doi: 10.1029/2004JF000149

Werner, B. T., & Kocurek, G. (1997). Bed-form dynamics: Does the tail wag the dog? *Geology*, *25*(9), 771–774. doi: 10.1130/0091-7613(1997)025⟨0771:BFDDTT⟩2.3.CO;2

Wilson, G. W., & Hay, A. E. (2016). Acoustic observations of near-bed sediment concentration and flux statistics above migrating sand dunes. *Geophysical Research Letters*, *43*(12), 6304–6312. doi: 10.1002/2016GL069579

Wong, M., & Parker, G. (2006). Reanalysis and Correction of Bed-Load Relation of Meyer-Peter and Müller Using Their Own Database. *Journal of Hydraulic Engineering*, *132*(11), 1159–1168. doi: 10.1061/(ASCE)0733-9429(2006)132:11(1159)

Wu, Z., Furbish, D., & FoufoulaGeorgiou, E. (2020). Generalization of Hop DistanceTime Scaling and Particle Velocity Distributions via a TwoRegime Formalism of Bedload Particle Motions. *Water Resources Research*, *56*(1). doi: 10.1029/2019WR025116

Figure 1.

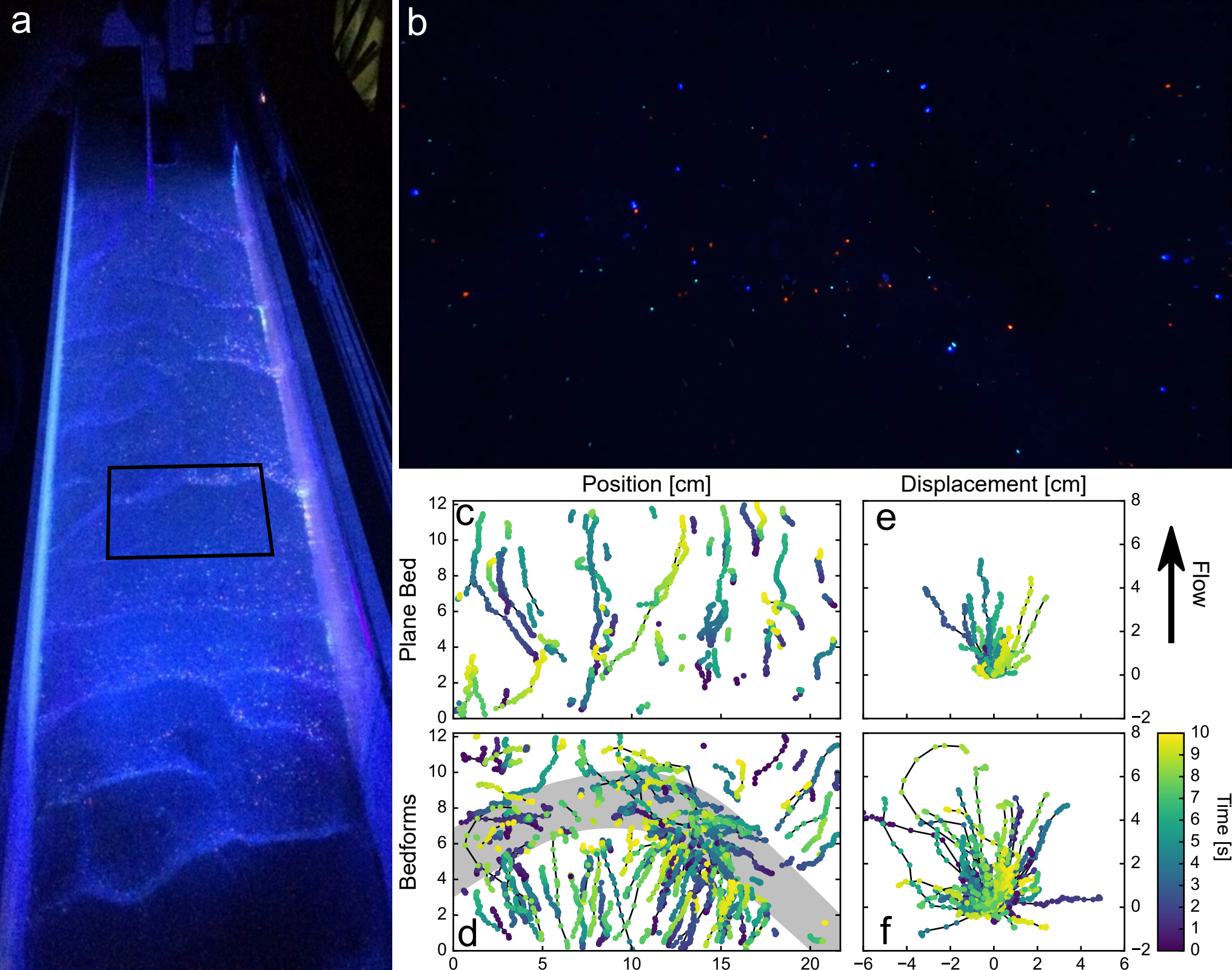
a
b
Position [cm]
Displacement [cm]
c
e
Plane Bed
Flow
d
f
Bedforms
Time [s]
0
5
10
15
20
−6
−4
−2
0
2
4
6
0
2
4
6
8
10
12
−2
0
1
2
3
4
5
6
7
8
9
10

Figure 2.

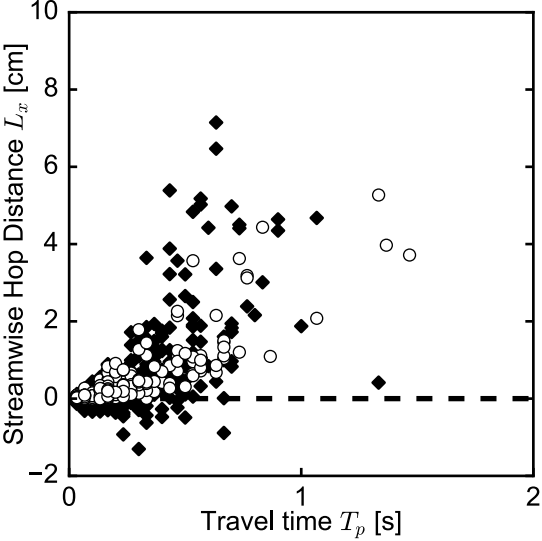
Streamwise Hop Distance L_x [cm]
Travel time T_p [s]

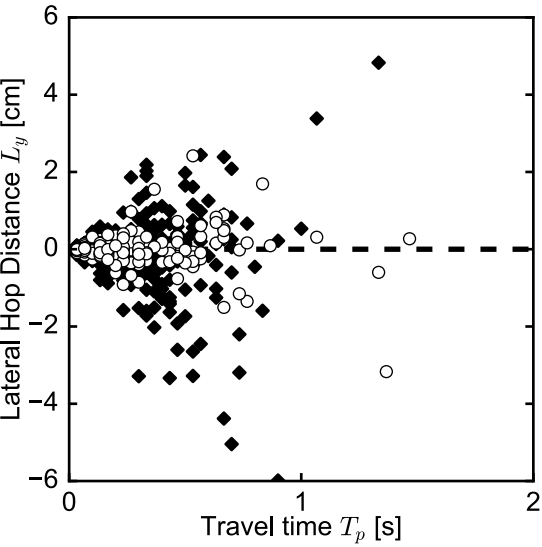
Lateral Hop Distance L_y [cm]
Travel time T_p [s]

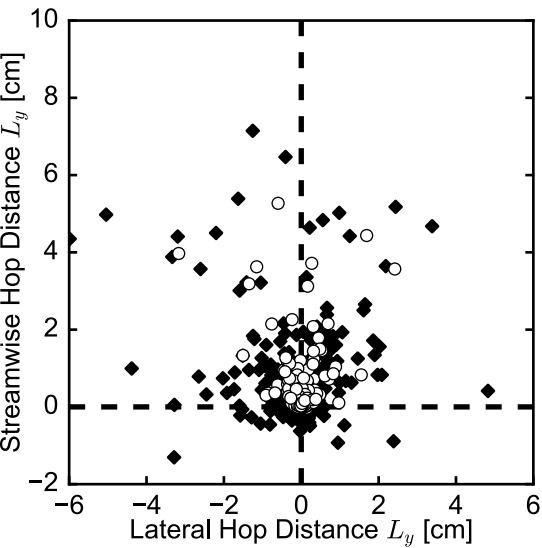
Streamwise Hop Distance L_y [cm]
Lateral Hop Distance L_y [cm]

Figure 3.

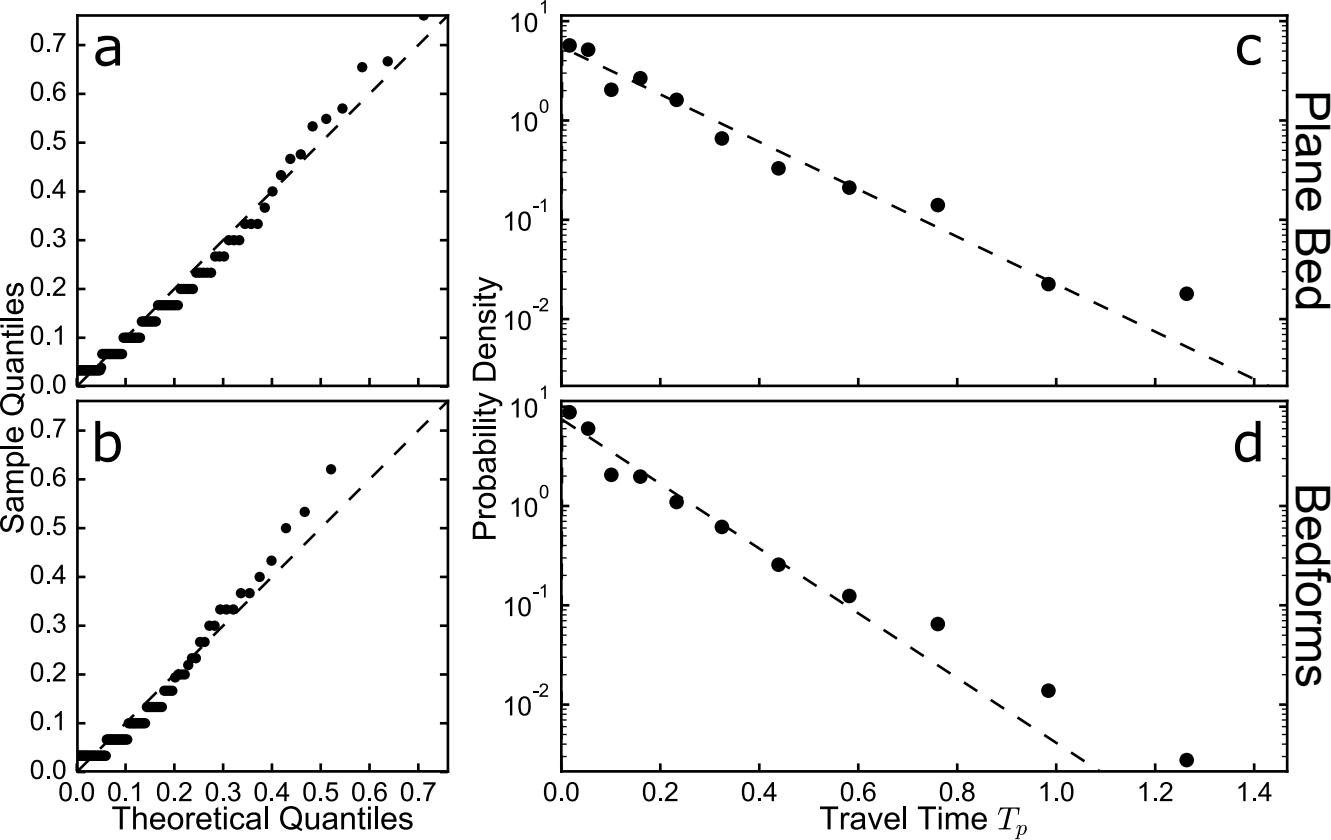
a
b
c
d
Plane Bed
Bedforms
Sample Quantiles
Theoretical Quantiles
Probability Density
Travel Time T_p
0.0
0.1
0.2
0.3
0.4
0.5
0.6
0.7
0.8
1.0
1.2
1.4
10^{1}
10^{0}
10^{-1}
10^{-2}

Figure 4.

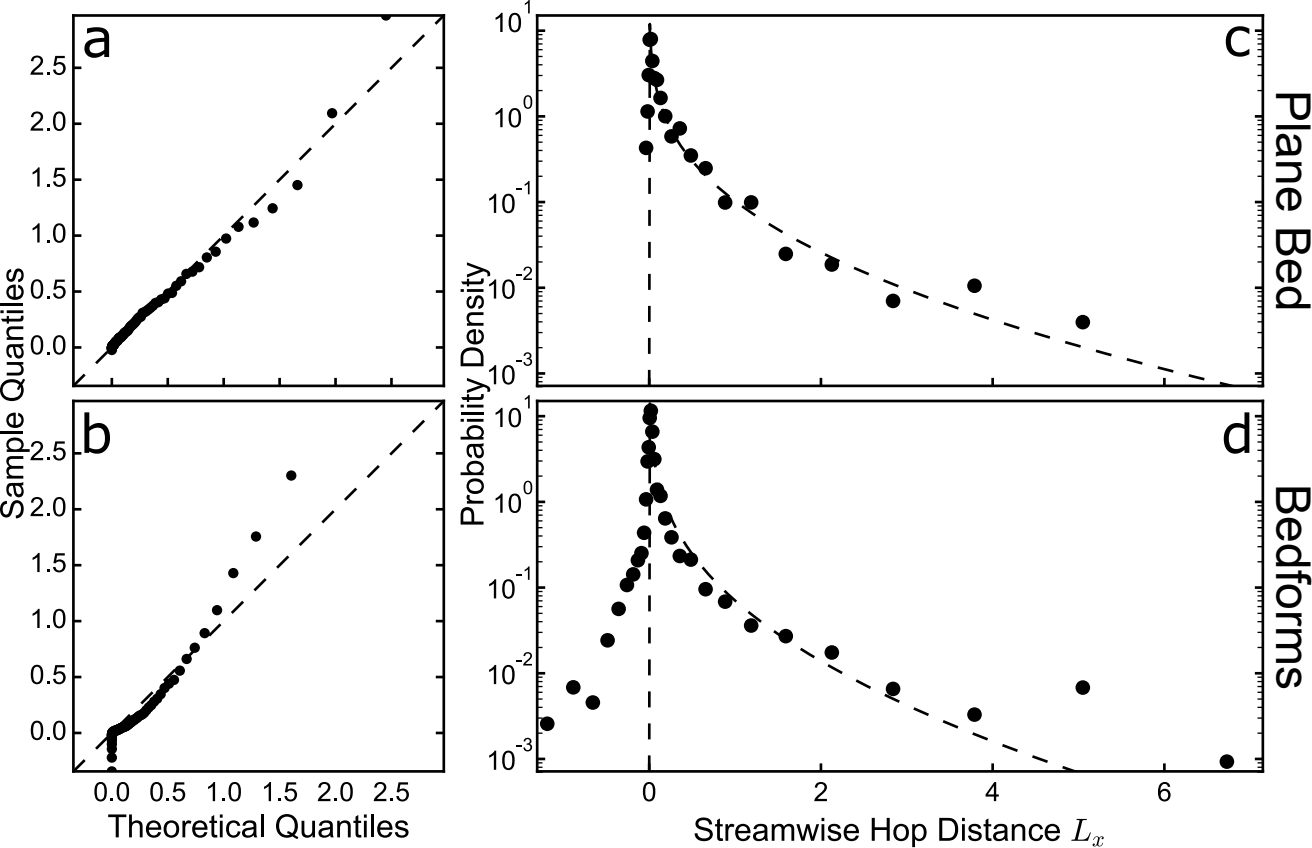
a
b
c
d
Plane Bed
Bedforms
Sample Quantiles
Theoretical Quantiles
Probability Density
Streamwise Hop Distance L_x
0.0
0.5
1.0
1.5
2.0
2.5
0
2
4
6
10^{1}
10^{0}
10^{-1}
10^{-2}
10^{-3}

Figure 5.

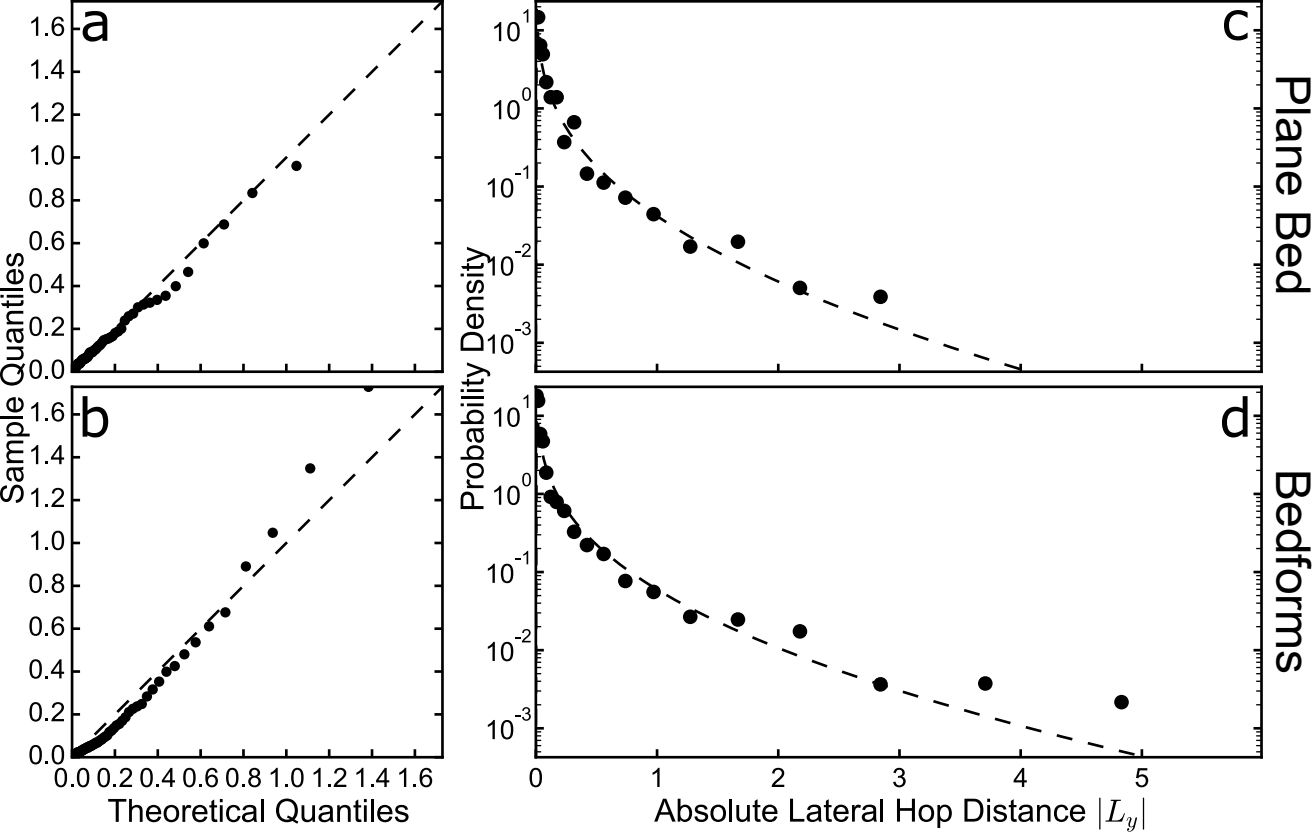
a
b
c
d
Plane Bed
Bedforms
Sample Quantiles
Theoretical Quantiles
Probability Density
Absolute Lateral Hop Distance $|L_y|$